Progress in Development for Helicon Plasma Thrusters by Use of the Rotating Electric Field (Lissajous Acceleration)

IEPC-2011-079

Presented at the 32nd International Electric Propulsion Conference,
Wiesbaden • Germany
September 11 – 15, 2011

Takeshi Matsuoka,[1] and Ikkoh Funaki[2]
Japan Aerospace Exploration Agency, Sagamihara, Kanagawa, 252-5210, Japan

Timofei. S. Rudenko,[3] Konstantin. P Shamrai[4]
Institute for Nuclear Research, Nauki, Kiev 03680, Ukraine

Shuhei SATOH,[5] and Takayasu. FUJINO[6]
University of Tsukuba, Tsukuba, Ibaraki, 305-8573, Japan

Takahiro Nakamura,[7] Kenji Yokoi,[8] Hiroyuki Nishida,[9] Shunjiro Shinohara[10]
Tokyo University of Agriculture and Technology, Koganei, Tokyo 184-8588, Japan

Tohru Hada,[11]
Kyushu University, Kasuga, Fukuoka 816-8580, Japan

and

Takao Tanikawa[12]
Tokai University, Hiratsuka, Kanagawa, 259-1292, Japan

Abstract: The Lissajous accelerator was shown to produce specific impulse (I_{sp}) as high as 10,000 s based on an analytical thrust model which consists of a particle trajectory analysis and an analytical model for an RF (i.e., Radio Frequency) electric field penetration into magnetized plasmas. Most critical condition of realization of such high I_{sp} is penetration of the RF electric field into the plasma. In this paper, the model for electric field penetration is described and a numerical benchmark with PIC (i.e., Particle in Cell) simulations is shown. As a first step toward verification of the thrust model, a plasma source of 26 mm diameter was fabricated at which the thrust model predicts few tens of % of the thrust by Lissajous

[1] Researcher Fellow, Institute of Space and Astronautical Science, takeshi.matsuoka1@gd.isas.jaxa.jp.
[2] Associate Professor, Institute of Space and Astronautical Science, funaki@isas.jaxa.jp.
[3] Graduate Student, Kiev National University, rudenkot@kinr.kiev.ua
[4] Head, Department of Plasma Theory, kshamrai@kinr.kiev.ua
[5] Graduate Student, Graduate School of Systems and Information Engineering, sato@fmm.kz.tsukuba.ac.jp
[6] Associate Professor, Graduate School of Systems and Information Engineering, tfujino@kz.tsukuba.ac.jp
[7] Graduate Student, Graduate School of Engineering, 50010643508@st.tuat.ac.jp
[8] Graduate Student, Graduate School of Engineering, 50009643303@st.tuat.ac.jp
[9] Associate Professor, Institute of Engineering, hnishida@cc.tuat.ac.jp
[10] Professor, Institute of Engineering, sshinoha@cc.tuat.ac.jp
[11] Professor, Interdisciplinary Graduate School of Engineering Sciences, hada@esst.kyushu-u.ac.jp
[12] Professor, Research Institute of Science and Technology, tnth@keyaki.cc.u-tokai.ac.jp

acceleration compared with the thermal thrust by electron thermal pressure (i.e., dominant competitor against Lissajous acceleration). Preliminary thermal thrust measurements for the plasma source shows that thrust of 2 mN and I_{sp} of 260 s with 2.1 kW input power to the RF circuit when the axial magnetic field is set at 80 G for Ar gas flow of 0.9 mg/s. And a projection based on the displacement by measured thermal thrust and estimated thrust by the thrust model suggests that noise reduction for the thrust stand is required in order to detect thrust increase due to Lissajous acceleration.

Nomenclature

A = areal density given by spatial integration of plasma density in a cross sectional plane of the thruster
B = magnetic field
E = electric field
F = thrust
L = distance between electrodes
R = radius
T = temperature
V = voltage
j = current density
k_β = Boltzmann constant
m = electron mass
$\dot{m}$ = mass flow rate
n = number density
q = dimensionless parameter for field penetration model
r_0 = thruster radius, plasma radius
s = sheath width
v = velocity
β = density gradient
γ = specific heat
ε = dimensionless parameter for field penetration model
ω = angular frequency
ω_{ce} = electron cyclotron frequency
ω_{LH} = lower hybrid frequency
ω_{pe} = electron plasma frequency

SUBSCRIPTS

E.M. = electromagnetic
D = drift
LH = lower hybrid
c = coil
e = electron
i = ion
th = thermal
0 = indicating constant

I. Introduction

A long lifetime electric propulsion is required to realize demanding missions such as sending orbiter to Jupiter's satellite. To meet this requirement, we initiated so called HEAT (Helicon Electrodeless Advanced Thruster) project whose goal is demonstrating specific impulse (I_{sp}) more than 4,000 s with a thrust power efficiency better than 50 % and operation duration of 1,000 hours.[1] The word "electrodeless" means that the no electrode has contact with plasmas. There are two keys for extending the lifetime. The first key is minimizing plasma contact with thruster structure such as wall of tubes, which hold plasmas, and electrodes. The second key is magnetoplasma acceleration which may not require neutralizers such as realized by VASIMR.[2] A long lifetime may be possible when a magnetic field is applied such that the plasma density is small at vicinity of the structure and energize plasma remotely. Thus

we adopted RF (radio frequency) fields for energizing plasmas: ionization and acceleration under a static magnetic field. Worldwide efforts have been devoted in order to develop such "electrodeless" thrusters: the VASIMR (Variable Specific Impulse Magnetoplasma Rocket),[2] HDLT (Helicon Double Layer Thruster),[3] mHT (Mini helicon thruster),[4] and the High Power Electrodeless Plasma Thruster.[5]

One of the plasma acceleration scheme in the HEAT project is the Lissajous method and was proposed by Toki et al.[6] The configuration of the thruster is shown in Fig. 1a. The thruster consists of three parts: the solenoid coil, the plasma production part, and the acceleration part. The solenoid coil is used to generate a flaring magnetic field. The plasma is produced by RF fields which are launched through the quartz tube by the plasma generation antenna. This type of plasma is known as helicon plasmas and provides higher densities than conventional method (e.g., inductively coupled plasmas) with robust discharge operations.[7-12] In the acceleration part, a rotating electric field (i.e., REF) is launched by use of planar antennae such that the electric field vector rotates in the transverse plane (i.e., $E_x = E_0 \cos \omega t$, $E_y = E_0 \sin \omega t$). When the frequency for the REF is in the range given by $\omega_{LH} << \omega << \omega_{ce}$, ions are immobile. Here ω_{LH} and ω_{ce} are the lower hybrid and the electron cyclotron frequencies. The REF drives azimuthal electron current through the electron E×B drift when the plasma radial density profile is peaked on the thruster axis as shown in Fig. 1b. The electromagnetic thrust is obtained as the repulsion force between the electron current and the coil current. We refer this type of thrust as the "E.M. thrust" in this paper. Preliminary estimation of the I_{sp} is shown to be 5,000 s for accessible parameter ranges in the experiments [13] and therefore we pursue the method.

The thrust can be produced from the helicon plasma alone. We refer this type of thrust as the "thermal thrust". Several groups reported thrust measurements for such thrusters: mHT,[4] HDLT,[14] PM-HDLT (Permanent Magnet Helicon Double Layer Thruster) [15], however the specific impulse has not reached competitive value against ion thrusters. Thrust power efficiency is estimated to be in between few % to few tens of % based on the published data [4,15] and also not enough for practical applications for space transportations. Such low efficiencies indicate the thruster may not be optimized and there is a room for further development. Note that there is ongoing debate for the thrust generation mechanism.[16-19] One of the mechanisms is thrust generation from electron thermal pressure acting on the end plate as shown in Fig. 1c. The thermal thrust is given by,

$$F_{th} = Ak_\beta T_e r_0^2 . \tag{1}$$

Here, the quantity A is given by an integral $A = \int n(x,y)dxdy$ in the cross sectional plane of the thruster with a density profile of $n(x,y)$. This formula is verified in experiments by use of PM-HDLT [15].

Development of the Lissajous method has not been matured but is at basic research status. The plasma flow velocity had been observed for several years with and without Lissajous acceleration but the increment of the Mach number with Lissajous acceleration compared with the velocity without the acceleration is much smaller than unity.[6, 20-22] In order to find conditions to maximize the E.M. thrust due to the Lissajous method, the analytical thrust model was developed[13, 23-25] and parameter survey by use of 2D PIC (e.g., Particle in Cell) simulations were performed.[21] Those works revealed that the thrust is proportional with a dimensionless parameter (R_D/r_0) and the thrust is expected to be maximum when R_D/r_0 is set at certain value (i.e., $R_D/r_0 \sim 0.4$).[13,21]

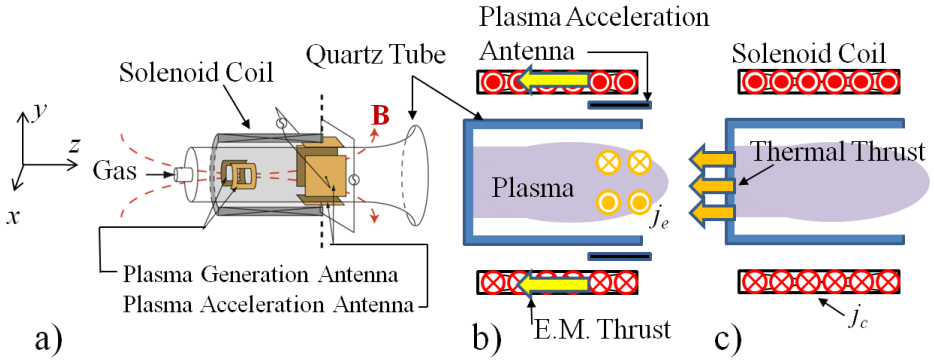

Figure 1. Conceptual diagram of Lissajous acceleration method. *a) Configuration, b) the E. M. thrust, and c) the thermal thrust,*

Here the parameter R_D and the thrust formula are given by,

$$R_D = \frac{E_0}{\omega B_z}, \tag{2}$$

The thrust is given by,

$$F_{E.M.} = \frac{\pi}{4} e\beta n_0 \omega B_z \left(\frac{R_D}{r_0}\right)^2 r_0^4 + \frac{\pi}{2}\beta n_0 k_\beta T_e r_0^2 . \tag{3}$$

Here, a parabolic shape density profile is assumed and is given by $n = \left\{1-\beta\left(r/r_0\right)^2\right\} n_0$. In the R.H.S. of Eq. (3), the first and the second terms are the thrust by the Lissajous acceleration and by diamagnetic current, respectively. The derivation of the thrust formula is reported in Refs. 13, 24.

We note here that there are ongoing debates for the physical processes of thrust generation, in particular with three topics: 1) electric field penetration into magnetized plasmas, 2) excitation of azimuthal electron current by a rotating electric field and 3) force transfer from the electron current to ions. The first topic affects the value of R_D since the plasma may shield externally applied electric field. Therefore, the electric field penetration into magnetized plasma is critical in order to apply Lissajous method for thrusters. An analytical model for RF electric field penetration into magnetized plasmas (i.e., the electric field penetration model) was developed and was bench marked by the PIC simulations.[23,24]

In order to find parameter range where the Lissajous acceleration method is competitive against ion or hall thrusters, a parametric survey of the Lissajous acceleration by use of the thrust model (i.e., Eq. (3)) was performed.[25] In this research, an optimum value (i.e., $R_D/r_0 = 0.4$) was used for the thrust model, which gives upper bound of potential performance, and showed that I_{sp} of 21,000 s with mass flow rate of 0.2 mg/s at $r_0 = 0.05$ m.[25] Other parameters are taken to be $\omega/2\pi = 10$ MHz, $B_z = 0.1$ T, $n_0 = 10^{17}$ m^{-3}, $\beta = 0.5$, $T_e = 10$ eV. The thrust and the thrust power for above mentioned values are 40 mN and 2.4 kW, respectively.

When thrust power efficiency of 50 % is realized, the propulsion system needs electrical power of 4.8 kW. This value is adequate for missions in next two decades from a technological point view of power supplies. It may be difficult to develop a power balance model which predicts the thrust power efficiency without feedback from experiments. In the thrust model and the electric field penetration model, no power loss processes are included. Therefore the experiments are required not only to confirm scaling laws for the thrust model but also obtain the thrust power efficiency. The thrust from thrusters by use of the Lissajous acceleration method has not been measured. Therefore we need to develop a laboratory model of the thruster which is suitable for the thrust measurement and a thrust stand.

In this paper, an analytical model for electric field penetration into magnetized plasmas and preliminary experiments, whose objectives are 1) developing a plasma source and 2) measuring the thermal thrust in order to find a lower limit of thrust measurements in our experimental conditions, are described. Outline of this paper is following. In section II, the electric field penetration model and its benchmark by PIC simulations are given. The future plans and discussions are also given for this topic. In section III, a scaling law is reviewed. The preliminary experiments and future plans for verifying the scaling law are also given. The summary is given to close the paper.

II. Electric Field Penetration

In this section, the electric field penetration model and benchmark by PIC simulations are described. Details of the model and simulations are given in future publications. The analytical model is found to be consistent with the PIC simulations in the assumed conditions with parameters which give $R_D/r_0 < 0.01$.

A. 1D Electrostatic Electric Field Penetration Model

Although the REF vector has two components, we consider only the E_x component in order to simplify the problem. A slab of neutral plasma [n_e (electron density) = n_i (ion density) = n_0 = constant] is placed between two planar electrodes as shown in Fig. 2. The distance between electrodes was set at L. Ion sheaths ($n_i = n_0$, $n_e = 0$) of variable widths are placed between the plasma and the electrodes. The system is immersed in a uniform ambient magnetic field of strength B_z. The Poisson equation is solved with assuming continuity conditions of the electric field. Plasma response is modeled by a uniform electron cold fluid with immobile ion background. Collisions are neglected for the sake of simplicity. The electrical field is driven by setting a time varying potential at each electrode,

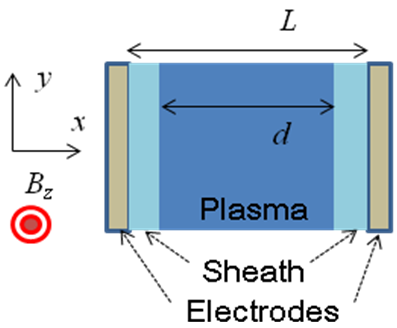

Figure 2. Configuration of field penetration model

$V(t) = V_0 \sin(\omega t)/2$ at the left electrode and $V(t) = -V_0 \sin(\omega t)/2$ at the right electrode, respectively. The ion matrix sheath model (n_e = 0 in the sheath) is assumed. The thickness of the sheath is obtained by solving a Newtonian motion equation for the electron fluid. The electric field in the plasma is obtained as $E_x(x,t) = E_{p0} \sin(\omega t)$,

$$\frac{E_{p0}}{V_0 / L} = \frac{2\varepsilon}{q}\left(\sqrt{\varepsilon^2 + q} - \varepsilon\right) \tag{4}$$

with $\varepsilon = 1 - \omega^2 / \omega_{ce}^2$. A dimensionless parameter q is defined by,

$$q = 8\frac{e}{m}\frac{\omega_{pe}^2}{\omega_{ce}^4}\frac{V_0}{L^2}. \tag{5}$$

Here, ω_{pe} is the plasma frequency given by density n_0. Note that the electric field in the plasma is uniform due to charge neutrality as one can see that the E_{p0} does not depend on x in Eq. (4). The amplitude of the field monotonically decreases with increase of q as shown in Fig. 3 by dashed curves. The dimensionless parameter of q is varied by changing the magnetic field for two densities. The other parameters in the figure are $\omega/2\pi$ = 100 MHz, V_0 = 10 V and L = 1 cm. The shape of the model curve is not sensitive to the difference of the plasma density. Note that the two theoretical curves overlap each other since Eq. (4) does not depend on plasma density explicitly but on q. However, q depends on plasma density and the density difference appears as different range of q in Fig. 3.

According to Eq. (4), the strong electric field is expected for a small value of q. and can reach the value without plasma (i.e., $E_{p0} = V_0/L$). The model curve is consistent with data points obtained by simulations described in next sub section.

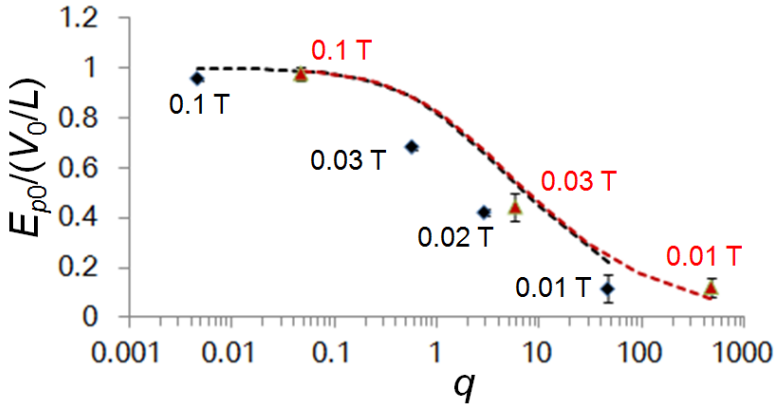

Figure 3. Electrical field strength as a function of q. *Simulation data points are shown for the plasma density of 10^{18} (10^{19}) m^{-3} by diamonds (triangles). The black (red) dotted curve shows electrical field strength from Eq. (4) for the plasma density of 10^{18} (10^{19}) m^{-3}. Strength of the magnetic field is shown in the plot for simulation data points.*

B. Benchmark by Particle in Cell Simulations

In order to verify Eq. (4), a series of 1D electrostatic simulation is performed by use of VORPAL code.* The configuration is shown in Fig. 1 which is identical as in the model. Identical parameters are used as in the model. The numerical time step and the spatial step are set at 1/10 of the plasma wave period and the Debye length, respectively. The simulation duration is 5 RF cycles and no significant particle loss is observed. The super particle number is varied from 200 (1,000) to 1,000 (10,000) for simulations at the density of 10^{18} (10^{19}) m^{-3} and the results are not affected by the number of the super particles. This indicates a negligible influence of numerical heating on

* http://www.txcorp.com/products/VORPAL/

simulation results. The Ar ions with a charge state of 1 with a real mass ratio to the electron are used in the simulation. The ion and electron temperatures are 0.3 eV and 5 eV, respectively. Both energy distribution functions are assumed to be Maxwellian distribution as an initial condition. The electric field in the simulation is obtained by a three-step post process. First, the REF strength is spatially averaged between 0.05L and 0.95L in order to avoid the strong electric field in the sheath region. Second, the spatially averaged electric field is Fourier transformed to obtain a frequency spectrum. The spectrum shows a peak at the drive frequency (100 MHz) except for a data point at ($n_0 = 10^{19}$ m^{-3}, B_{z0} = 0.01 T) where the intensity at the drive frequency is comparable with the intensity in the noise region described below. Third, the spectral peak is divided by the value which corresponds to the electrical field (V_0/L) without the plasma. The error bar is estimated by taking averaged spectral intensity in a frequency range between 500 MHz to 1 GHz.

C. Future Plan of Analysis and Discussions

In this section, four factors which are not included in the field penetration model are discussed.

1) The parameters used in the PIC simulations give $R_D/r_0 < 0.01$. Whereas the thrust model shows that the thrust increases with R_D/r_0 as shown by Eq. (3) and therefore, equation (4) should be verified for parameters which give greater value of R_D/r_0.

2) In order to obtain the E.M. thrust by the Lissajous method, a radial density profile should be peaked on axis such as a parabolic shape as shown by Eq. (3). However, in the field penetration model, we assumed uniform plasmas. The influence of the spatial non uniformity on the field penetration should be studied. Other spatial inhomogeneity such as gradient in the z direction would affect field pattern of the REF and therefore the thrust.

3) In order to verify the excitation of azimuthal electron current, multidimensional analysis is essential. An analytical model for field penetration is under development for the 2D planar configuration.

4) In this analysis, collisions are neglected, and therefore, the influence due to collisions for the field penetration is unknown. Collisions may affect thrust due to Ohmic heating. When the REF amplitude is increased, the Ohmic heating will be increased and therefore the electron temperature would increase. The rise of the electron temperature increases the thermal thrust as can be seen by Eq. (1). Therefore influence of collisions should be studied.

5) Other sources of thrust, in particular ponderomotive force, should be taken into account.

III. Status of Experiments and Future Plans

In this section, the thrust model is reviewed and selected parameters for experiments are described with its reasons. The preliminary experiments for the thermal thrust measurements and future plans for the E.M. thrust measurements are described.

A. Review of Thrust Model and Selected Parameters

In order to verify the thrust model, we decided to confirm thrust scaling on the thruster radius. The thrust as a function of thruster radius (r_0) from Eq. (1), (3) is shown in Fig. 4. The E.M. thrust by the Lissajous acceleration exceeds the thermal thrust when the thruster radius is greater than ~ 0.01 m for fixed other parameters. Therefore, selecting three thruster radiuses as shown in Fig. 4 are selected for verifying the thrust model.

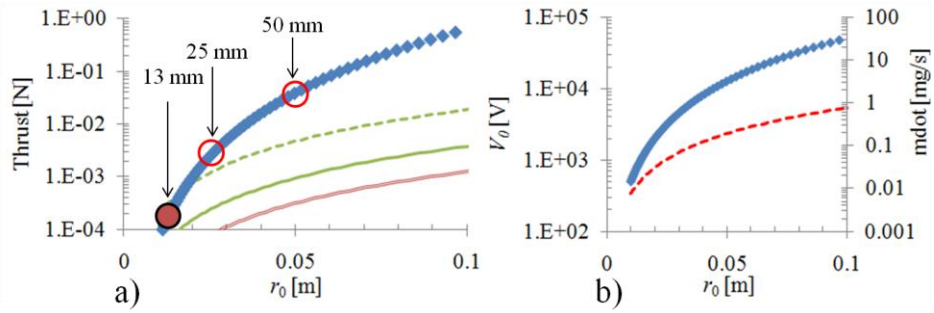

Figure 4. Scaling Laws. *a) Thrust, and b) required voltage and mass flow rate as a function of r_0. The magnetic field is B_z = 0.1 T. Curves in (a) are for the thrust due to the Lissajous acceleration (diamond), due to diamagnetic current (double line). Thermal thrust is shown for the electron temperature of T_e (solid line) and 5 T_e (dashed line). T_e is set at 10 eV. Curves in (b) are the required voltage (diamond) and the mass flow rate (dashed line).*

Absolute value of thrust should be known to select a proper type of thrust measurement technique. Following parameters are selected, i.e.,

$$n_0 = 10^{17}\ \mathrm{m}^{-3},\ R_D/r_0 = 0.4,\ \beta = 0.5,\ T_e = 10\ \mathrm{eV},\ f_{\mathrm{RF}} = 10\ \mathrm{MHz}. \quad (6)$$

Here, the density is selected by two reasons, 1) keeping thrust power in a range of reasonable value (e.g., order of kW), 2) avoiding collisions which are not taken into account in the thrust model.

The $\beta = 0.685$ is estimated from a measured radial density profile in helicon plasmas whose parameters were $n_0 = 3.7\times10^{16}\ \mathrm{m}^{-3}$, $T_e = 7$ eV, $f_{\mathrm{RF}} = 27.12$ MHz, $B_z = 0.095$ T, input power of 290 W for plasma production and 125 W for Lissajous acceleration in experiments.[22] Note that the observation location is 50 mm (c.f. 26 mm tube) downstream from the exit of the quartz tube, and therefore the plasma density and β are expected to be different. The value of β is taken to be arbitral number based on those experiments.

The electron temperature is also arbitrary set at 10 eV based on the those experiments.*

The RF frequency for the REF is set to 10 MHz by considering a tradeoff relation for required voltage applied to the RF acceleration antennae and the thrust as explained bellow. In the range of the magnetic field under consideration (i.e., $0.05 < B_z < 0.1$ T), q is in a range between 0.05 and 0.006 which is small enough to achieve almost 100 % penetration of the electric field. Required potential difference between planar electrodes is shown in Fig. 4b and is given by,[24]

$$V_0 = 2\frac{m}{e}\frac{R_D}{r_0}\omega_{ce}\omega r_0^2 + 2\frac{m}{e}\left(\frac{R_D}{r_0}\right)^2\frac{\omega_{pe}^2\omega^2}{\omega_{ce}^2}r_0^2 \cdot \quad (7)$$

For the parameter range of the consideration, first term of the R.H.S. is dominant and the voltage is proportional to B_{z0} and ω but does not depend on n_0. In this limit, the thrust can be increased with ω and B_{z0} until the available voltage, which RF power supply could provide, is achieved. The required voltage increases from 0.5 kV to 12.4 kV when the radius is varied from 0.01 m to 0.05 m with fixed $B_z = 0.1$ T. We note that the peak voltage applied to each electrode is half of the value estimated by Eq. (7) which is several kV because of that four RF power supplies are considered to provide RF voltage to four planar antennae in order to generate the REF. This several kV of peak voltage may be adequate and therefore requirements for the power supplies may be tolerable. Decreasing the RF frequency reduces the voltage whereas the thrust is decreased since the thrust is proportional with RF frequency as indicated by Eq. (3). Therefore we set the frequency at 10 MHz which is in the assumed range of $\omega_{LH} << \omega << \omega_{ce}$ in the thrust model.

The expected E.M. thrust is indicated by circles in Fig. 4a. Total thrust (i.e., $F_{total} = F_{E.M.} + F_{th}$) is in the range between 0.28 mN and 40 mN. Note that the thrust can be increased by increasing the density (i.e., mass flow rate) as long as q is kept small because of that the thrust is proportional to the density as shown in Eq. (3). When the plasma density is increased to $10^{18}\ \mathrm{m}^{-3}$, the thrust is increased by ten times whereas required voltage remains almost the same because of that q is so small (0.06) that almost full penetration of the electric field is expected from Eq. (4). This value gives the basis for the experimental design in particular the selection of the type of a thrust stand.

B. Preliminary Experiments: Thermal Thrust Measurements

The experimental set up consists of 6 parts 1) vacuum chamber, 2) solenoid coil, 3) an RF system, 4) a quartz tube, 5) a gas feed system and 6) a pendulum type thrust stand.

For 1) and 2), the "Large Helicon Plasma Device" (LHPD) [8-10] is used and is shown in Fig. 5a. A cylindrical shape vacuum chamber whose inner diameter of 0.738 m and the axial length of 4.86 m are pumped by a turbomolecular pump at a pumping speed of 1800 l/s. The chamber pressure was 10^{-4} Pa without gas feed and was kept bellow 0.006 Pa with Ar gas feed up to 0.9 mg/s. Note that the pressure is measured before the discharge. The main coil is indicated in Fig. 5a which consists of 14 coils and provides an axial magnetic field to the thruster. The magnetic field is calibrated at the location of the quartz tube by use of a Hall probe. The strength and the direction of the magnetic field were varied by changing the current and its direction in the main coils. It should be noted that the solenoid coil is outside of the thrust stand and therefore the E.M. thrust cannot be measured. Hence the thrust measured in those preliminary experiments is the thermal thrust.

* This electron temperature is higher than the typical helicon plasmas in the literatures, and therefore, the thermal thrust may be overestimated. However, use of the overestimated thermal thrust is safe since we seek the parameter range where the E.M. thrust is greater than the thermal thrust.

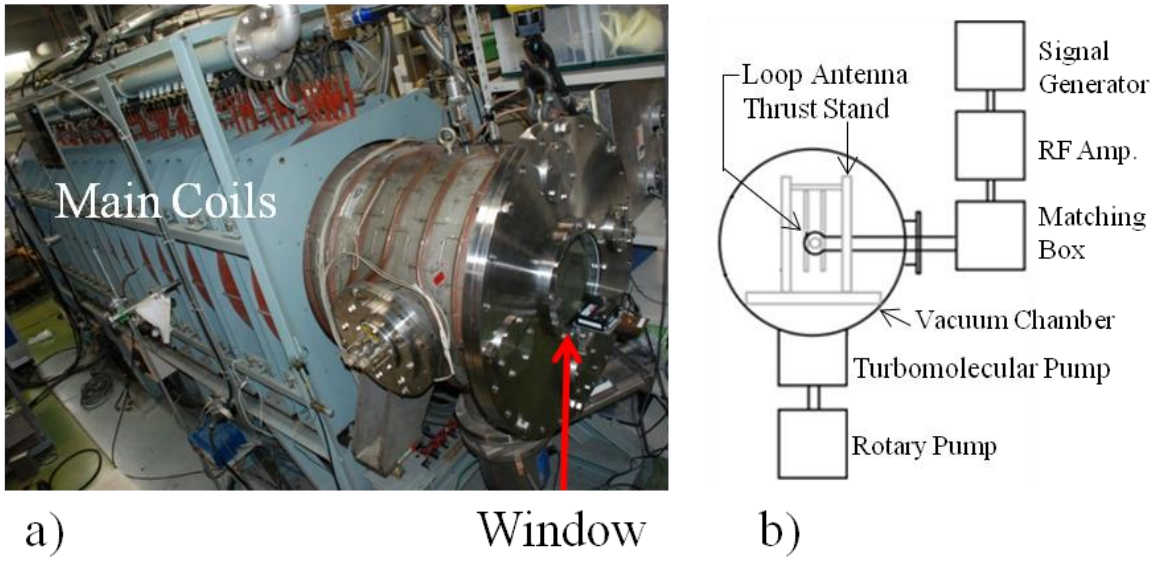

Figure 5. Experimental setup. *a) Vacuum chamber and main coil of LHPD, b) Schematic diagram of RF setup.*

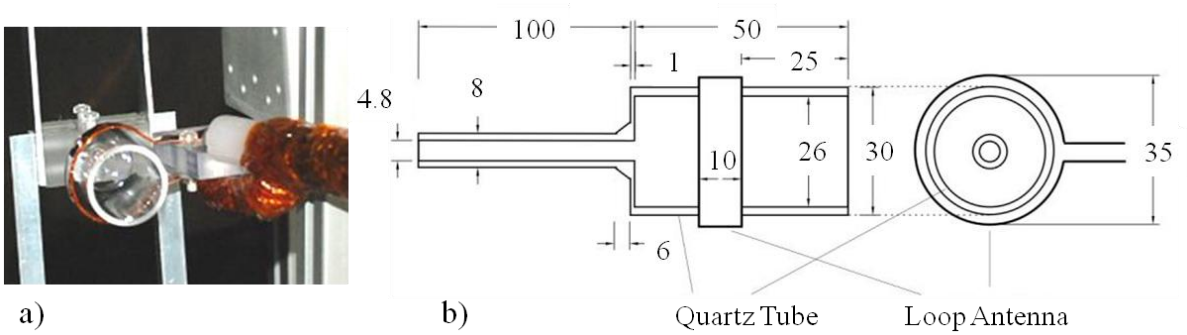

Figure 6. Quartz tube 26 mm ID and loop antenna. *a) Picture and b) dimensions in mm.*

For 3), the schematic diagram of the RF system is shown in Fig. 5b. An RF signal at 9.5 MHz from the signal generator is amplified up to ~2 kW of power (average power) and then sent to a matching box. We found that the frequency of 9.5 MHz showed a minimum return loss (~ 40 dB) by use of a network analyzer for tuning the matching box. The amplified RF signal is sent through an RF vacuum feedthrough (not shown in Fig. 5b) and a coaxial cable (i.e., 0.7 m of RG-17A/U) to a loop antenna. We operate the RF system in a pulse mode in order to avoid heating the RF system and the thruster structure. The envelope of the RF pulse is a step function with duration of 50 ms. We estimate input power by subtracting reflection power from forward power. The reflection and the forward power were measured by two directional couplers installed in the RF amplifier.

For 4), we picked a quartz tube whose dimensions are the radius of 0.013 m and the length of 0.05 m for inner volume as shown in Fig. 6b. The reason to use this size is that this radius had been used in previous Lissajous acceleration experiments and plasma parameters are well characterized in TUAT (Tokyo University of Agriculture and Technology).[6, 26] The quartz tube was placed at 80 cm from the surface of the end port flange of the chamber. Here the distance is measured from the open edge of the quartz tube. Note that the loop antenna does not have physical contacts with the quartz tube in order to avoid the stiffness of the cable which prevents the motion of the thrust stand.

For 5), a schematic diagram of the gas feed system is shown in Fig. 7. Ar gas was fed by use of a mass flow controller of STEC-E440J whose full scale is set at 30 sccm for Ar. The narrow end of the quartz tube is inserted to a PVC tube (SWAGELOCK, LT-4-6) whose dimensions are ID 1/4" and OD 3/8". The other end of the PVC tube was connected to the vacuum gas feedthrough. It is important to place the PVC tube along the arm of the pendulum in order to avoid the drift of the thruster due to stiffness of the PVC tube as shown in Fig. 7b.

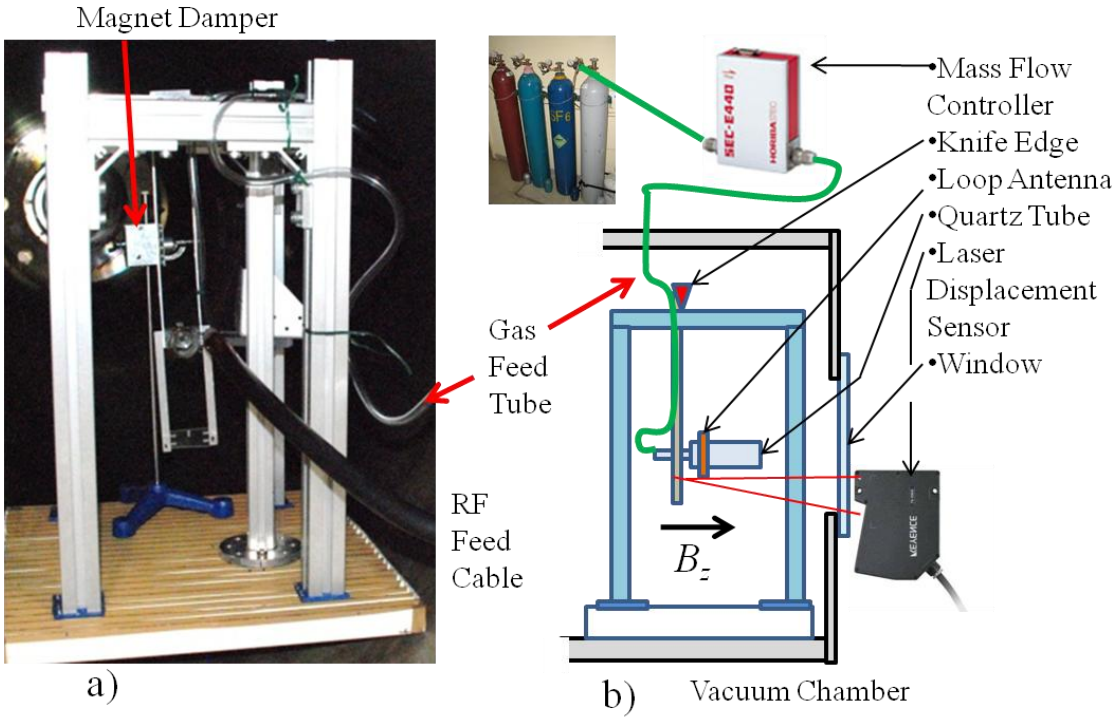

Figure 7. Thrust stand and gas feed system. *a) Picture of thrust stand and b) schematic diagram of gas feed system.*

For 6), the pendulum type thrust stand is installed in the vacuum chamber as shown in Fig. 7. An Al knife edge was used to provide a line contact to the supporting structure. A magnet damper was used to damp the oscillation motion. The displacement of the pendulum was detected by a laser displacement sensor (KEYENCE, LK-G500). The natural periods of the pendulum is approximately 1 s and is much longer than the RF pulse duration. Therefore the impulse due to thermal thrust acting on the pendulum stand can be considered to be infinite small duration. The displacement is calibrated by striking an iron ball of 0.52 g to the pendulum. Figure 8 shows the output of the laser displacement sensor from the experimental parameters shown in table I. The sign of the B_z is defined in the Fig. 7b. The impulse is applied approximately at the time of 41 s in Fig. 8. A curve fitting method by use of a theoretical formula for damped oscillations was used to retrieve the applied impulse by the thruster. The thrust is calculated by dividing the impulse by the duration of the RF pulse.

Figure 9 shows the image of plasma emission captured by a digital CCD camera with identical experimental conditions of table I. Here, exposure conditions for the image and inset are different. The central bright area in the image corresponds to the narrow part of the quartz tube.

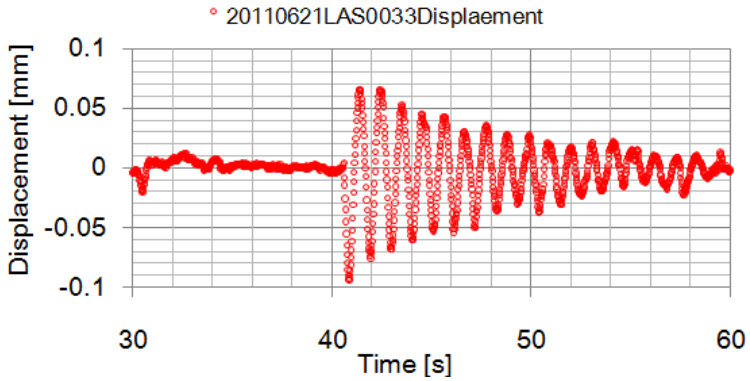

Figure 8. Output of laser displacement sensor.

Table I. Experimental Parameters.

$\omega/2\pi$	9.5 MHz
Input Power	2.0 kW (Otherwise Stated)
Duration of RF Pulse	50 ms
Chamber Pressure Before Discharge	$< 6\times10^{-3}$ Pa
B_z	-0.008 T (Otherwise Stated)
Mass Flow Rate of Ar	0.6 mg/s (Otherwise Stated)

Sign of the magnetic field is defined in Fig. 7b.

The thermal thrust was proportional with the mass flow rate for B_z = -0.008 T and -0.015 T with fixed other parameters as shown in Fig. 10. The plasma emission becomes brighter with increase of the mass flow rate. Note that the exposure condition for images in Fig. 10 was fixed. When the positive magnetic field (i.e., B_z = 0.008 T) was applied, 2 ± 0.2 mN of thrust was observed at mass flow rate of 0.9 mg/s. The increase of the thrust compared with the negative B_z could be explained by the increase of the input power. Shot averaged power for B_z = -0.008 T and B_z = 0.008 T are 2.0 ± 0.1 kW and 2.1 ± 0.1 kW, respectively. Absorbed power by the plasma should be less than the input power due to a circuit loss. The analysis for the absorbed power by the plasma is under progress. Those observations suggest that the increase of the thrust with the increase of plasma density as is expected from Eq. (1). We plan to measure the plasma density in future experiments.

The specific impulse can be estimated from the slope of the linear fitting curve to the data points as shown in Fig. 10 by use of the relation, $F_{th} = \dot{m} I_{sp} g$. The estimated I_{sp} is 180 s, 94 s, and 260 s for B_z = -0.008 T, -0.015 and 0.008 T, respectively. The shot averaged input power was 2.0 ± 0.1 kW for data points shown in Fig. 10. The difference of the I_{sp} may be due to difference of absorbed power by plasmas.

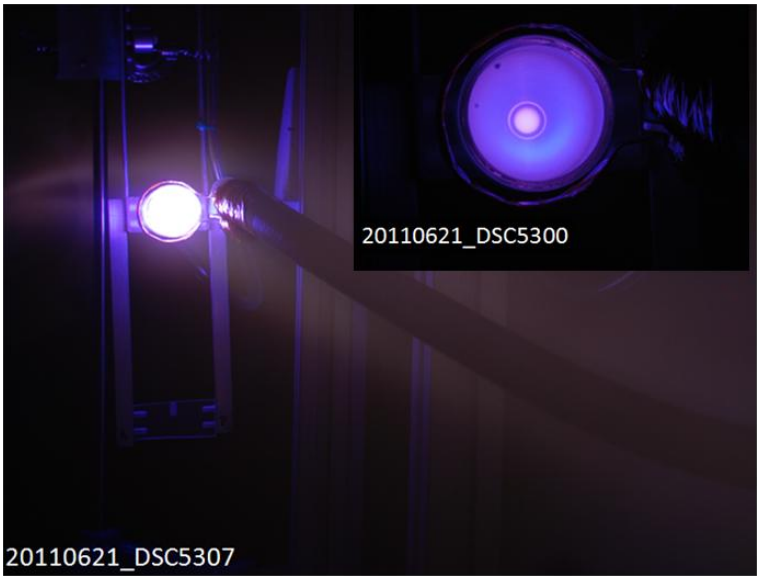

Figure 9. Image of plasma emission. *Inset : Zoom up of the quartz tube during discharge.*

The dominant contribution of error bar comes from the error associated with the curve fitting method for the impulse calibration. The 54 % of the error bar is due to this error. The fitting error for experimental data is less than 10 % of the error bar. This difference could be explained by the influence of an air flow since the calibration was performed in the atmosphere but the experimental data was obtained in vacuum. This result indicates that the pendulum type thrust stand can be used to detect as low as a few mN but improvement is required for detecting thrust by the Lissajous method.

C. Future Plans and Design of Laboratory Models

In order to measure the E.M. thrust, a permanent magnet should be on the thrust stand. We decided to use the permanent magnet in order to reduce weight of the thruster and avoiding heating problems. This requires reduction of the error since the estimated E.M. thrust by the thrust model is 0.3 mN* and may be too small to detect. The weight of the thruster will be increased at least ten times due to permanent magnets. When the weight is increased

*Note that the thrust can be increased by the increase of the mass flow rate which consequently increases plasma density. Another way of increasing sensitivity of the thrust measurement is increasing the RF pulse duration since the displacement is expected to be proportional with the duration. However, the duration should be kept below 10 % of the natural cycle of the oscillation in order to apply the formulae of damped oscillations.

by ten times, the displacement is reduced by ten times and therefore the displacement could be ~ 10 microns. The reduced displacement is too small for current configuration because of the vibration of the thrust stand (~ 20 microns) which can be seen in Fig. 8 before the oscillations. Note that the displacement of approximately 100 microns corresponds to the thrust of 1.1±0.3 mN for Fig. 8. Therefore the vibration must be reduced at least ten times from current configuration such that the thrust increment by the E.M. thrust of 0.3 mN can be detected. Two solutions for reducing the vibrations are considered: 1) placing displacement sensor inside the chamber and 2) replacing the pendulum type thrust stand by a torsion type one. The error associated with the calibration is a major contribution as it was discussed in the previous section. Therefore, calibration procedure must be improved in order to reduce noise.

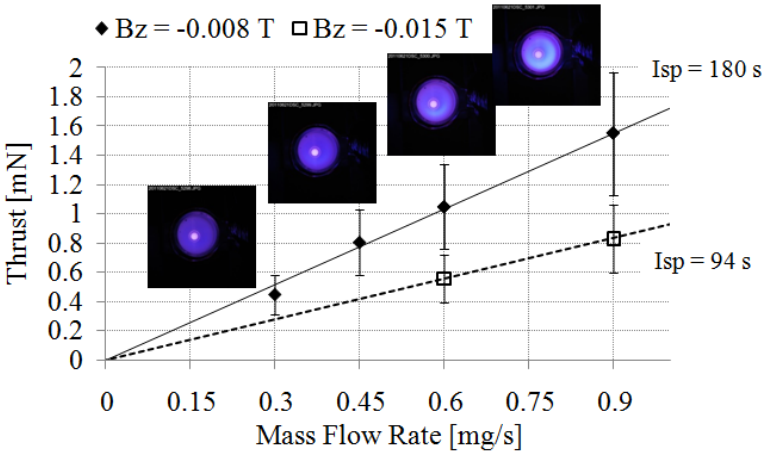

Figure 10. Correlation of emission brightness from plasma and thrust. *Diamonds and squares are data points for B_z = 0.008 T and B_z = 0.015 T, respectively. Other experimental parameters are shown in Table I. Error bar includes uncertainty of impulse calibration, shot to shot fluctuation and error of the curve fitting. Each data point is the average of 2-3 shots.*

IV. Summary

In this paper, the analytical model for electric field penetration in the electrostatic limit is described which is used in order to clarify the parameter range where a high electrical field is available for the Lissajous acceleration method. A dimensionless parameter q which represents electrical field shielding by magnetized plasmas is introduced. The electrical field strength obtained from the model was consistent with those of the 1D particle in cell (PIC) simulations. Estimated values from PIC simulations show a good agreement with the model prediction.

Preliminary experiments of thermal thrust measurements from a 26 mm ID plasma source are reported. The first plasma is successfully ignited. The developed pendulum type thrust stand was tested by measuring thermal thrust from the plasma source. The thrust was found to be proportional with the mass flow rate and greater thrust was observed for weaker axial magnetic field. The thrust was 2 mN with 2.1 kW input RF power with I_{sp} of 260 s. It is found that the sensitivity of the thrust stand is not enough for detecting the E.M. thrust which is estimated by the thrust model. Those experimental findings will be used for future experiments in order to confirm the thrust scaling and to study thruster efficiency.

Acknowledgments

This work is supported by the Grants-in-Aid for Scientific Research under Contract No. (S) 21226019 from the JSPS.

References

[1]Shinohara, S., Nishida, H., Yokoi, K., Nakamura, T., Tanikawa, T., Hada, T., Otsuka, F., Motomura, T., Ohno, E., Funaki, I., Matsuoka, T., Shamrai, K. P., and Rudenko, T. S., "Research and Development of Electrodeless Plasma Thrusters Using High-Density Helicon Sources: The Heat Project", *32nd International Electric Propulsion Conference*, IEPC-2011-056, Sept.11-15, Wiesbaden, Germany, Sept. 2011.

[2]Chang Diaz, F. R., "The VASIMR Rocket," Scientific American, November 2000, Vol. 283, No. 5, 2000, pp., 90, 97.

[3]Charles, C., and Boswell, R., "Current-free double-layer formation in a high density helicon discharge," *Applied Physics Letters*, Vol. 82, 2003, pp., 1356, 1358.

[4]Batishchev, O., "Minihelicon Plasma Thruster," *IEEE Transactions on Plasma Science*., Vol. 37, No. 8, 2009, pp., 1563, 1571.

[5]Emsellem, G. D., and Larigaldie, S., "Low Power Behavior of the High Power Electrodeless Plasma Thruster," *44th AIAA/ASME/SAE/ASEE Joint Propulsion Conference & Exhibit*, 21-23 July 2008, Hartford, CT, AIAA 2008-5009.

[6]Toki, K., Shinohara, S., Tanikawa, T., Shamrai, K. P., and Funaki, I., "Preliminary Investigation of Helicon Plasma Source for Electric Propulsion Applications," *28th International Conference on Electric Propulsion*, IEPC-2003-0168, Toulouse, 2003.

[7]Boswell, R. W., "Plasma production using a standing helicon wave," *Physics Letters*, Vo. 33A, No. 7, 1970, pp., 457, 458.

[8]Shinohara, S., Hada, T., Motomuta, T., Tanaka, K., Tanikawa, T., Toki, K., Tanaka, Y., and Shamrai, K. P., "Development of High-Density Helicon Plasma Sources and Their Applications," *Physics of Plasmas*, Vol. 16, 2009, pp., 057104-1, 057104-9.

[9]Shinohara, S., and Tanikawa, T., "Development of very large helicon plasma source," *Review of Scientific Instruments*, Vol. 75, No. 6, 2004, pp., 1941, 1946.

[10]Tanikawa, T., and Shinohara, S., "Plasma performance in very large helicon device," *Thin Solid Films*, Vol. 506-507, 2006, pp., 559, 563.

[11]Shamrai, K. P., and Shinohara, S., "Modeling electromagnetic field excitation and rf power absorption in a large helicon plasma," *Thin Solid Films*, Vol. 506-507, 2006, pp., 555,558.

[12]Motomura, T., Tanaka, K., Shinohara, S., Tanikawa, T., and Shamrai, K. P., "Characteristics of Large Diameter, High-Density Helicon Plasma with Short Axial Length Using a Flat Spiral Antenna," *Journal of Plasma and Fusion Research SERIES*, Vol.8, 2009, pp., 6,10.

[13]Toki, K., Shinohara, S., Tanikawa, T., Hada, T., Funaki, I., Tanaka, Y., Yamaguchi A. and Shamrai K. P., "A Study of Electrodeless MPD Thruster Using Helicon Plasma Source," JAXA special publication JAXA-SP-08-013, JAXA 2009-02-27, JAXA-SP-08-013, ISSN, 1349-113X, AA0064241013 in Japanese.

[14]West, M. D., Charles, C., and Boswell, R. W., "Space Simulation Testing of the Helicon Double Layer Thruster Prototype," *46th AIAA/ASME/SAE/ASEE Joint Propulsion Conference & Exhibit* 25 - 28 July 2010, Nashville, TN, AIAA2010-7016.

[15]Takahashi, K., Lafleur, T., Charles, C., Alexander, P., Boswell, R. W., Perren, M., Laine, R., Pottinger, S., Lappas, V., Harle, T., and Lamprou, D., "Direct thrust measurement of a permanent magnet helicon double layer thruster," *Applied Physics Letters*, Vol. 98, 2011, pp., 141503-1, 141503-3.

[16]Fruchtman, A., "Electric Field in a Double Layer and the Imparted Momentum," *Physical Review Letters*, Vol. 96, 2006, pp., 065002-1, 065002-4.

[17]Liberman, M. A., and Charles, C., "Theory for Formation of a Low-Pressure, Current-Free Double Layer," *Physical Review Letters*, Vol. 97, 2006, pp., 045003-1, 045003-4.

[18]Chen, F. F., "Physical mechanism of current-free double layers," *Physics of Plasmas*, Vol. 13, 2006, pp., 034502-1, 034502-3.

[19]Fruchtman, A., "Neutral Depletion in a Collisionless Plasma," *IEEE Transactions on Plasma Science*., Vol. 36, No. 2, 2008, pp., 403, 413.

[20]Toki, K., Shinohara, S., Tanikawa, T., Hada, T., Funaki, I., Shamrai, K. P., Tanaka, Y. and Yamaguchi, A., "Plasma Acceleration in a Compact Helicon Source Using RF Antennae," *J. Plasma Fusion Res. SERIES*, Vol. 8, 2009, pp., 25, 30.

[21]Nishida, H., Shinohara, S., Tanikawa, T., Hada T., Funaki I., Matsuoka T., Shamrai, K. P., and Motomura, T., "Preliminary Study on Electrodeless Magneto-Plasma-Dynamic Thruster Using a Helicon Plasma Source," *46th AIAA/ASME/SAE/ASEE Joint Propulsion Conference & Exhibit*, AIAA-2010-7013, Nashiville, 2010.

[22]Nakamura, T., Yokoi, K., Nishida, H., Shinohara, S., Funaki, I., Matsuoka, T., Tanikawa, T., Hada, T., Shamrai, K. P., and Rudenko, T. S., "Experimental Investigation of Plasma Acceleration by Rotating Electric Field for Electrodeless Plasma Thruster", *32nd International Electric Propulsion Conference*, IEPC-2011-279, Sept.11-15, Wiesbaden, Germany, Sept. 2011.

[23]Matsuoka, T., Funaki, I., Nakamura, T., Yokoi, K., Nishida, H., Rudenko, T. S., Shamrai, K. P., Tanikawa T., Hada T. and Shinohara, S., "Scaling Laws of Lissajous Acceleration for Electrodeless Helicon Plasma Thruster," *Plasma Fusion Research Special Issue on ITC20*, (to be published).

[24]Matsuoka, T., Nakamura, T., Yokoi, K., Rudenko, T. S., Funaki, I., Nishida, H., Shamrai, K. P., Tanikawa, T., Hada, T. and Shinohara, S., "Electric Field Penetration in Electrodeless Helicon Plasma Thruster," *28th International Symposium on Space Technology and Science* , ISTS-2011-b-09, Ginowan, Okinawa, Japan, 2011.*

[25]Satoh, S., Matsuoka, T., Fujino, T. and Funaki, I., "A Theoretical Analysis for Electrodeless Lissajous Acceleration of HELICON Plasmas," *42nd AIAA Plasmadynamics and Lasers Conference*, AIAA-2011-4008, Honolulu, 2011.†

[26]Toki, K., Shinohara, S., Tanikawa, T., Shamrai, K.P., "Small helicon plasma source for electric propulsion," *Thin Solid Films*, Vol. 506-507, 2006, pp., 597, 600.

* The formula of the thermal thrust (i.e., $F_{th} = \pi(1-\beta/2)(\gamma+1)n_0 k_\beta T_e r_0^2$) in this reference must be replaced by $F_{th} = \pi(1-\beta/2)n_0 k_\beta T_e r_0^2$. The values in the text are obtained by the corrected formula.

† Same as the footnote *.